The American Journal of Pathology, Vol. 171, No. 3, September 2007

DOI: 10.2353/ajpath.2007.061199

Epithelial and Mesenchymal Cell Biology

Leukocytes Induce Epithelial to Mesenchymal Transition after Unilateral Ureteral Obstruction in Neonatal Mice

Bärbel Lange-Sperandio,*† Agnes Trautmann,* Oliver Eickelberg,‡ Aparna Jayachandran,‡ Stephan Oberle,* Florian Schmidutz,* Barbara Rodenbeck,* Meike Hömme,* Richard Horuk,§ and Franz Schaefer*

From the Department of Pediatrics, Ruprecht-Karls-University, Heidelberg, Germany; the Department of Pediatrics,† Ludwig-Maximilians-University, Munich, Germany; the Department of Medicine II,‡ University of Giessen, Giessen, Germany; and the Department of Immunology,§ Berlex Biosciences, Richmond, California*

Urinary tract obstruction during renal development leads to tubular apoptosis, tubular atrophy, and interstitial fibrosis. Epithelial to mesenchymal transition (EMT) has been proposed as a key mechanism of myofibroblast accumulation in renal fibrosis. We studied the interplay of leukocyte infiltration, tubular apoptosis, and EMT in renal fibrosis induced by unilateral ureteral obstruction (UUO) in neonatal mice. We show that leukocytes mediate tubular apoptosis and EMT in the developing kidney with obstructive nephropathy. Blocking leukocyte recruitment by using the chemokine receptor-1 antagonist BX471 protected against tubular apoptosis and interstitial fibrosis, as evidenced by reduced monocyte influx, a decrease in EMT, and attenuated collagen deposition. EMT was rapidly induced within 24 hours after UUO along with up-regulation of the transcription factors Snail1 and Snail2/Slug, preceding the induction of α-smooth muscle actin and vimentin. In the presence of BX471, the expression of chemokines, as well as of Snail1 and Snail2/Slug, in the obstructed kidney was completely attenuated. This was associated with reduced macrophage and T-cell infiltration, tubular apoptosis, and interstitial fibrosis in the developing kidney. Our findings provide evidence that leukocytes induce EMT and renal fibrosis after UUO and suggest that chemokine receptor-1 antagonism may prove beneficial in obstructive nephropathy. ***(Am J Pathol 2007, 171:861–871; DOI: 10.2353/ajpath.2007.061199)***

Congenital obstructive nephropathy is a frequent cause of kidney failure in infants and children.[1] Chronic unilateral ureteral obstruction (UUO) leads to interstitial inflammation, tubular apoptosis, and interstitial fibrosis.[2–4] Central to these events is the influx of macrophages and lymphocytes into the tubulointerstitium.[5–7] Macrophages release proinflammatory cytokines, cytotoxic substances, and induce apoptosis in tubular cells.[8–10] Furthermore, macrophages are critical in promoting extracellular matrix production and fibroblast proliferation.[8,11,12]

Recently, it has been shown that fibroblasts at sites of inflammation originate either from the bone marrow or from an epithelial to mesenchymal transition (EMT) of tubular cells at sites of injury.[13,14] This process of EMT is characterized by the loss of epithelial adhesion, polarity, and epithelial cell-specific markers such as E-cadherin.[15,16] In addition, cells undergoing EMT gain the expression of fibroblast (vimentin) and smooth muscle [α-smooth muscle actin (α-SMA)] markers. These changes lead to an intermediate mesenchymal phenotype, termed the myofibroblast, which is motile and invasive and produces extracellular matrix.[13,17,18] Molecular markers for EMT include loss of E-cadherin, increased expression of vimentin and SMA, nuclear localization of activated β-catenin, and increased production of the transcription factors Snail1 and Snail2/Slug.[15] Snail1 acts as a key regulator of EMT by suppressing E-cadherin transcription, increasing matrix metalloproteinases, and modulating tight junction protein expression.[15,19,20] Snail2/Slug inhibits E-cadherin production,[21] thereby facilitating detachment of epithelial cells, thus enabling them to migrate.[21,22] Both Snail1 and Snail2 are crucial in the initiation and progression of EMT.[15,23] Growth factors including transforming growth factor-β_1 (TGF-β_1), fibroblast growth factor-2, and epidermal growth factor have been found to induce EMT.[23–25] TGF-β_1 stimulates extracellular matrix

Supported by the German Research Foundation (stipend La 1257/2-2 to B.L.-S.).

Accepted for publication June 19, 2007.

Address reprint requests to Bärbel Lange-Sperandio, M.D., Pediatric Nephrology Division, Dr. v. Haunersches Kinderspital, Ludwig-Maximilians-University, Lindwurmstr.4, 80337 München, Germany. E-mail: baerbel.lange-sperandio@med.uni-muenchen.de.

production and is released by tubular cells and infiltrating macrophages after UUO.[26,27]

Macrophage and T-cell recruitment in UUO is mediated via adhesion molecules and chemokines.[5,28–30] Chemokines are small chemotactic cytokines that direct leukocyte recruitment in inflammation and homeostasis through ligation of chemokine receptors. CC chemokines interact with their specific chemokine receptors (CCRs) on intravascular leukocytes and guide these cells into the interstitial compartment.[31] To study the contribution of infiltrating leukocytes to EMT and interstitial fibrosis in congenital obstructive nephropathy, we performed UUO in newborn mice. Because glomeruli continue to form postnatally in mice, neonatal UUO at the second day of life is a model to study the effects of urinary tract obstruction on renal development.[3,32] Newborn mice were subsequently treated with BX471, a small nonpeptide CCR-1 antagonist that specifically blocks interstitial leukocyte recruitment.[5,30,33–35] We found that BX471 reduced the amount of infiltrating macrophages and T cells, production of renal CCL5, CCL3, and CCL4, tubular apoptosis, and interstitial fibrosis after UUO. In addition, blockade of leukocyte recruitment prevented EMT via attenuation of early transcription factors (Snail1 and Snail2) and reduction of active β-catenin, translating into reduced renal expression of vimentin and SMA in the developing kidney with UUO. Together, these data argue for a significant contribution of infiltrating leukocytes to EMT and the progression of interstitial fibrosis. We show for the first time that EMT is present in the developing kidney with UUO. Our data demonstrate that macrophages are necessary for disease progression and that CCR-1 antagonism protects neonatally obstructed developing kidneys from EMT and interstitial damage.

Materials and Methods

Experimental Protocol

Two-day-old wild-type mice (C57BL/6) were distributed into four groups ($n = 16$ in each group) receiving subcutaneous injections of either BX471 (Berlex Biosciences, Richmond, CA) at 100 mg/kg body weight per day dissolved in propylene glycol (vehicle) for 5 (days 2 to 7 of life) or 12 days (days 2 to 14 of life) or vehicle once daily. BX471 was dissolved in propylene glycol (no. 39,803-9, 1,2-propanediol; Aldrich, Seelze, Germany) at a concentration of 25 mg/ml. Mice were subjected to complete left ureteral obstruction or sham operation under general anesthesia with isoflurane and oxygen at the 2nd day of life as described before.[7] After recovery neonatal mice were returned to their mothers until sacrifice 5 and 12 days after surgery (at days 7 and 14 of life; $n = 8$ per group). The experimental protocol was approved by the Committee for Animal Experimentation of the University of Heidelberg.

Determination of Pharmacokinetic Parameters

The pharmacokinetic profile of BX471 was examined in neonatal mice. Mice were subcutaneously dosed with BX471 (100 mg/kg body weight) in vehicle. BX471 was dissolved in propylene glycol at a concentration of 25 mg/ml. Blood samples (10 μl) were taken by cardiac puncture at 1, 3, 6, 12, and 24 hours after injection of BX471 ($n = 4$ per time point).

Identification of Infiltrating Leukocytes, CCL5, Snail1, and α-SMA

Infiltration of leukocytes was examined by immunohistochemistry.[7] Four percent paraformaldehyde-fixed, paraffin-embedded sections were subjected to antigen retrieval and incubated with either rat anti-mouse monoclonal F4/80 antibody (supernatant from F4/80 hybridoma cells; American Type Culture Collection, Manassas, VA) against monocytes/macrophages or rat anti-mouse CD3 antibody (Serotec, Oxford, UK) against T lymphocytes. For CCL5 expression, a polyclonal rabbit anti-mouse antibody (PeproTech, London, UK) was used. EMT immunostaining was performed using antibodies against Snail1 (Abcam Inc., Cambridge, MA) at 1:200 and α-SMA (Sigma, Munich, Germany) at 1:500. Specificity was assessed through simultaneous staining of control sections with a nonspecific, species-controlled primary antibody or preincubation of the primary antibody with blocking peptides where available. Biotinylated goat anti-rat IgG or goat anti-rabbit IgG (Southern Biotechnology Associates, Inc., Birmingham, AL) were used as secondary antibodies. The sections were incubated with ABC reagent (Vectastain; Vector Laboratories, Burlingame, CA) and counterstained with methylene blue, hemalaun, or hematoxylin. Digital images of the sections ($n = 8$ in each group) were superimposed on a grid, and the number of grid points overlapping dark brown macrophages or CD3-positive lymphocytes in cortex and medulla was recorded for each field. Twelve nonoverlapping high-power fields at $\times$400 magnification were analyzed in a blinded manner. Data were expressed as the mean score $\pm$ SE per 12 high-power fields. Representative photomicrographs of macrophages, T-lymphocyte infiltration, CCL5, Snail1, and α-SMA expression in the obstructed kidney are shown in Figures 2, A–D, K, and L, and 7.

Detection of Apoptosis

Apoptotic cells were detected by the terminal deoxynucleotidyl transferase (TdT)-mediated dUTP-biotin nick-end labeling (TUNEL) assay.[36] Briefly, formalin-fixed tissue sections were deparaffinized and rehydrated in ethanol followed by incubation with proteinase K (20 μg/ml). After quenching, equilibration buffer was applied, followed by working strength enzyme (ApopTag Peroxidase In Situ Apoptosis Detection Kit; Intergen, Purchase, NY). Cells were regarded as TUNEL-positive if their nuclei were stained brown and displayed typical apoptotic

Table 1. Real-Time RT-PCR Primer Sequences

Gene	Forward primer	Reverse primer	Size (bp)
18S	5′-AGTTGGTGGAGCGATTTGTC-3′	5′-GCTGAGCCAGTTCAGTGTAGC-3′	205
TGF-β_1	5′-GGAACTCTACCAGAAATATAGCAACAATTC-3′	5′-TGTATTCCGTCTCCTTGGTTCAG-3′	141
Collagen I	5′-CTGGCGGTTCAGGTCCAA-3′	5′-GCTTCCCCATCATCATCTCCATTC-3′	73
CCL5	5′-CCAATCTTGCAGTCGTGTTTGT-3′	5′-CATCTCCAAATAGTTGATGTATTCTTGAAC-3′	98
CCL2	5′-ACCGTCAGTCAGTTGGTATCAAAG-3′	5′-CCGGATCTTAAAATTCTT-3′	105
CCL3	5′-CCAGCCAGGTGTCATTTTCCT-3′	5′-TCCAAGACTCTCAGGCATTCAGT-3′	116
CCL4	5′-CTCCAAGCCAGCTGTGGTATTC-3′	5′-CTCCAAGTCACTCATGTACTCAGTGA-3′	97

morphology. Tubular apoptosis in each kidney was calculated by counting the number of TUNEL-positive tubular cells in 12 sequentially selected fields at ×400 magnification and expressed as the mean number ± SE per 12 high-power fields. Representative photomicrographs are shown in Figure 2, E and F.

Measurement of Tubular Atrophy

Kidney sections were stained with periodic acid-Schiff for assessment of tubular basement membranes, and tubular atrophy was determined as described previously.[37] Atrophic tubules were identified by their irregular, thickened, and sometimes duplicated basement membranes. The number of atrophic tubules per field at ×400 magnification was counted, and 12 fields per kidney were analyzed ($n = 8$ per group). Representative photomicrographs are shown in Figure 2, G and H.

Morphometric Evaluation of Interstitial Fibrosis

Interstitial collagen deposition was measured in Masson trichrome-stained sections.[38] Digital images of the sections were superimposed on a grid, and the number of grid points overlapping interstitial blue-staining collagen was recorded for each field. Twelve nonoverlapping fields at ×400 magnification were analyzed in a blinded manner ($n = 8$ per group). Representative photomicrographs are shown in Figure 2, I and J.

Real-Time Quantitative Reverse Transcriptase-Polymerase Chain Reaction (RT-PCR)

In addition, 48 neonatal mice received BX471 treatment (days 2 to 14 of life) or vehicle and underwent UUO surgery or sham operation at the 2nd day of life for RT-PCR analysis. Kidneys were harvested 1, 5, and 12 days after obstruction at days 3, 7, and 14 of life ($n = 4$ in each group). RNA was isolated using TRI reagent (Sigma), checked for integrity on an agarose gel, and quantified photometrically. One μg of total RNA was reverse-transcribed using oligo(dT)/random hexamer primers (10:1). Real-time RT-PCR was performed using the ABI Prism 7000 real-time PCR system (Applied Biosystems, Darmstadt, Germany) with specific primers for 18S, TGF-β_1, collagen I, CCL5, CCL2, CCL3, and CCL4 (Table 1) and Universal Mastermix (also Applied Biosystems) with SYBR Green to detect PCR products at the end of each amplification step. Serial dilutions of an arbitrary cDNA pool were used to establish a standard curve. mRNA levels were normalized to corresponding 18S quantities determined within the same run. RT-PCR for analysis of EMT was performed using Go *Taq* Flexi DNA polymerase (Promega, Madison, WI). After an initial incubation at 95°C for 2 minutes, reactions consisted of 25 cycles of 94°C for 1 minute, (57°C, 58°C, and 60°C, as indicated below) for 1 minute, and 72°C for 30 seconds. The last cycle was followed by a 5-minute incubation at 72°C. The following primers were used to amplify the depicted products: GAPDH, α-SMA, vimentin, E-cadherin, Snail1, and Snail2/Slug (Table 2).

Western Immunoblotting

In addition, 36 neonatal mice received BX471 treatment (days 2 to 14 of life) or vehicle and underwent UUO surgery or sham operation at the second day of life for Western blot analysis. Kidneys were harvested 1, 5, and 12 days after obstruction ($n = 3$ in each group), homogenized in protein extraction buffer (1% Triton X-100, 100 mmol/L Tris, 100 mmol/L $Na_4P_2O_3$, 100 mmol/L NaF, and 10 mmol/L ethylenediamine tetraacetic acid) containing a cocktail of proteinase and phosphatase inhibitors (1 mmol/L Na_3VO_4, 1 mmol/L phenylmethyl sulfonyl fluoride, 10 μg/ml leupeptin, and 10 μg/ml aprotinin), and centrifuged for 60 minutes at 20,000 × g. Fifty μg of protein were separated on polyacrylamide gels at 180 V for 45 minutes and blotted onto nitrocellulose membranes (105 V, 80 minutes). After blocking for

Table 2. RT-PCR Primer Sequences

Gene	Forward primer	Reverse primer	Size (bp)
GAPDH	5′-AACTTTGGCATTGTGGAAGG-3′	5′-ACACATTGGGGGTAGGAACA-3′	223
SMA	5′-AGACAGCTATGGGGGGATG-3′	5′-GAAGGAATAGCCACGCTCAG-3′	451
Vimentin	5′-CGCAGCCTCTATTCCTCATC-3′	5′-AGCCACGCTTTCATACTGCT-3′	693
E-Cadherin	5′-AGTTTACCCAGCCGGTCTTT-3′	5′-AGGGTTCCTCGTTCTCCACT-3′	602
Snail1	5′-CACCCTCATCTGGGACTCTC-3′	5′-GCCAGACTCTTGGTGCTTGT-3′	604
Snail2/Slug	5′-AACATTTCAACGCCTCCAAG-3′	5′-CAGTGAGGGCAAGAGAAAGG-3′	631

1 hour in Tris-buffered saline with Tween 20 containing 5% nonfat dry milk, blots were incubated with primary antibodies at 4°C overnight. Blots were washed with Tris-buffered saline with Tween 20 and incubated with horseradish peroxidase-conjugated secondary antibody for 1 hour at room temperature. Immune complexes were detected using enhanced chemiluminescence (Amersham Pharmacia Biotech, Freiburg, Germany). Blots were exposed to X-ray films (Kodak, Stuttgart, Germany), and protein bands were quantified using densitometry. Each band represents one single mouse kidney. Rabbit anti-Snail1 antibody (antibody 17732; 1:1000) was purchased from Abcam (Cambridge, UK). Mouse anti-vimentin antibody (clone V9, V-6630, 1:200) was obtained from Sigma. Mouse anti-α-smooth muscle actin antibody (MO851; 1:200) was purchased from DAKO (Hamburg, Germany). Mouse anti-β-catenin (05-665, 1:200) was obtained from Upstate (Biomol, Hamburg, Germany). Mouse anti-E-cadherin antibody (BD 610182, 1:3000; Transduction Laboratories, Lexington, KY) was obtained from Becton Dickinson, Heidelberg, Germany.

Immunofluorescence

E-Cadherin expression in obstructed kidneys was examined by immunohistochemistry. Four percent paraformaldehyde-fixed, paraffin-embedded sections were subjected to antigen retrieval and incubated with rabbit anti-mouse E-cadherin (BD 610182, 1:2500 dilution; Transduction Laboratories) for 1 hour, washed extensively, and exposed to Cy3-labeled goat anti-rabbit IgG. Fluorescence was examined by fluorescence microscopy.

Statistical Analysis

Data are presented as mean ± SE. Comparisons between groups were made using one-way analysis of variance followed by the Student-Newman-Keuls test. Comparisons between left and right kidneys were performed using the Student's *t*-test for paired data. Statistical significance was defined as $P < 0.05$.

Results

Leukocyte Recruitment

UUO resulted in a significant and progressive increase in interstitial macrophage infiltration in all obstructed kidneys compared with sham-operated controls and intact opposite kidneys (Figure 1A). Mice treated with BX471 (from day 2 to day 14) showed a reduction of interstitial F4/80-positive macrophages by 48% at day 5 (190 ± 8 versus 359 ± 6, $P < 0.05$) (Figures 1A and 2, A and B) and by 35% at day 12 after UUO (332 ± 7 versus 507 ± 11, $P < 0.05$) compared with vehicle-treated controls (Figure 1A). Notably, also intact opposite kidneys demonstrated a significant reduction in macrophage infiltration under CCR-1 blockade at day 5 after obstruction (92 ± 4 versus 137 ± 5, $P < 0.05$) (Figure 1A). T-lymphocyte infiltration into the obstructed kidney increased significantly after UUO (Figure 1B). BX471 reduced the infiltration of CD3-positive T lymphocytes by 56% at day 5 (14.9 ± 1.1 versus 33.6 ± 2, $P < 0.05$) (Figures 1B and 2, C and D) and by 37% at day 12 of obstruction compared with vehicle-treated mice (94.5 ± 3.3 versus 151 ± 1.5, $P < 0.05$) (Figure 1B).

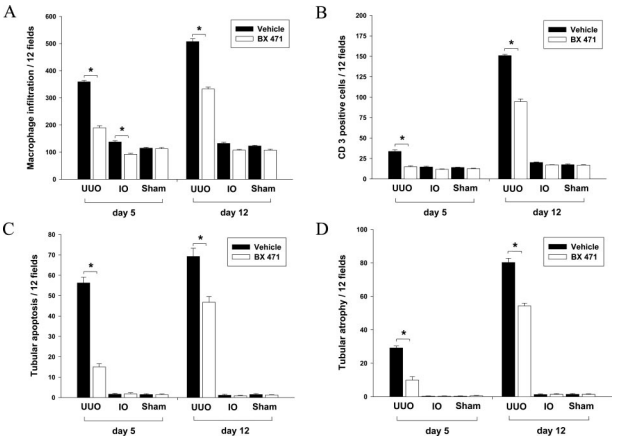

Figure 1. Morphometric analysis of renal macrophage infiltration (F4/80 antibody) (**A**), CD3-positive T-lymphocyte accumulation (CD3 antibody) (**B**), tubular apoptosis (TUNEL) (**C**), and tubular atrophy (**D**) at 5 and 12 days after obstruction in BX471-treated mice (d2 to d14) and vehicle-treated controls. Twelve fields were analyzed. UUO, obstructed kidney; IO, intact opposite kidney; sham, sham-operated control. Data are the mean ± SE ($n = 8$ in each group). *$P < 0.05$. Original magnifications, ×400.

Tubular Apoptosis

Tubular apoptosis was significantly increased in all obstructed kidneys when compared with intact opposite kidneys and sham-operated controls at days 5 and 12 after obstruction (Figure 1C). BX471-treated mice demonstrated a marked decrease in tubular apoptosis by 73% at day 5 (15 ± 1.6 versus 56.3 ± 2.7, $P < 0.05$) (Figures 1C and 2, E and F) and by 33% at day 12 after UUO (46.7 ± 2.8 versus 69.3 ± 4, $P < 0.05$) when compared with vehicle-treated controls (Figure 1C).

Tubular Atrophy

Tubular atrophy in the obstructed kidney was detectable at day 5 after UUO (Figure 1D). At 12 days after obstruction, there was a dramatic increase in thickened and sometimes duplicated tubular basement membranes in mice with UUO. Blockade of leukocyte recruitment by BX471 led to a significant reduction of tubular atrophy by 66% at day 5 after UUO (9.9 ± 2.1 versus 29.1 ± 1.2, $P < 0.05$) and by 32% at day 12 after obstruction compared with vehicle-treated controls (54 ± 1.6 versus 80 ± 2.5, $P < 0.05$) (Figures 1D and 2, G and H). Intact opposite kidneys and sham-operated controls had no signs of tubular atrophy (Figure 1D).

Interstitial Fibrosis

In all obstructed kidneys at 5 and 12 days after obstruction, interstitial collagen was markedly increased in the interstitial space compared with intact opposite kidneys

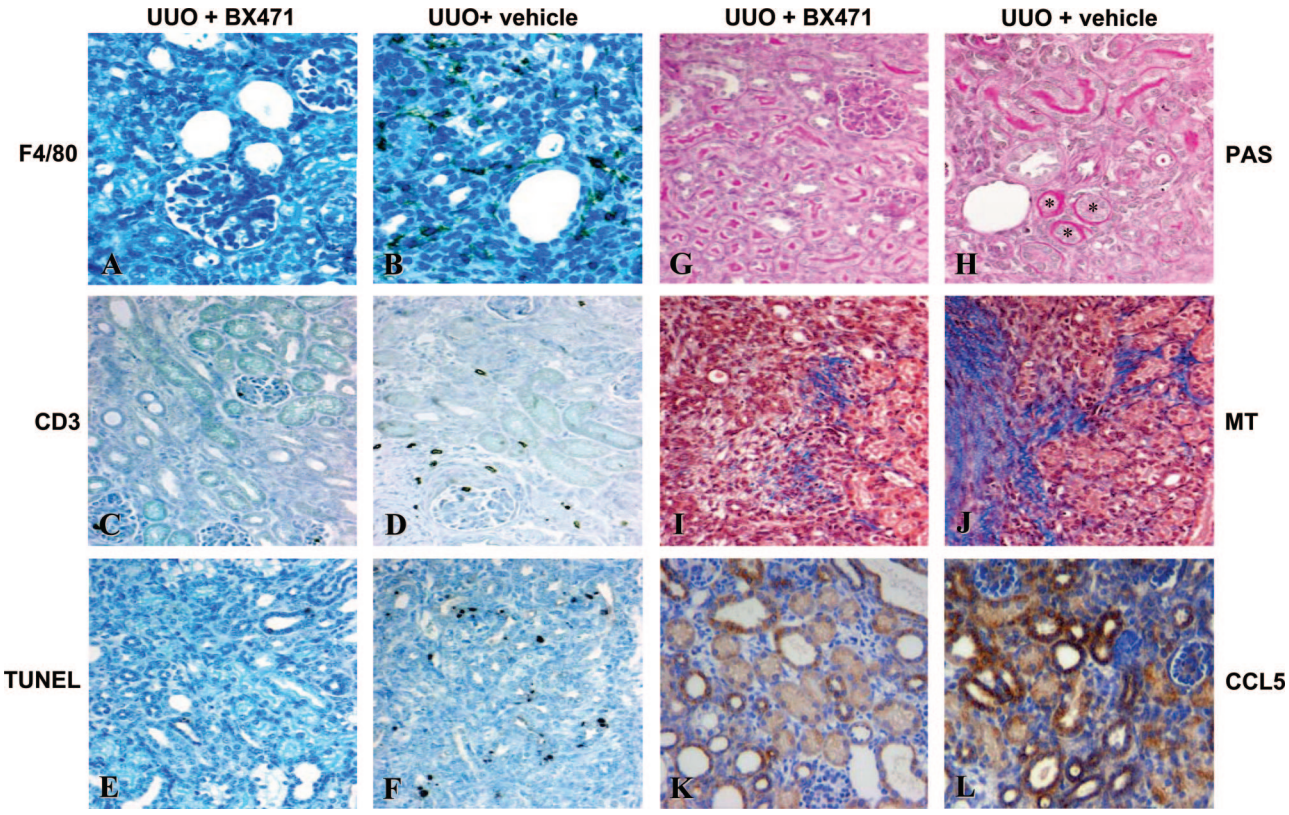

Figure 2. Representative photomicrographs of obstructed kidneys. Renal sections were stained for macrophage infiltration (F4/80 antibody) at 5 days after obstruction (UUO) in BX471-treated (**A**) and vehicle-treated mice (**B**). Neonatal mice received BX471 or vehicle from day 2 to day 14 of life. **A:** BX471-treated mice showed significantly fewer macrophages (black). Renal accumulation of CD3-positive T lymphocytes was reduced in the BX471-treated group (**C**) compared with vehicle-treated mice (**D**) at 5 days after UUO. Tubular apoptosis (TUNEL) at 5 days after obstruction in BX471-treated mice (**E**) and control mice (**F**), showing less TUNEL-positive tubular cells in the BX471-treated mouse kidney. Periodic acid-Schiff staining identified the thickened, irregular tubular basement membrane characteristic of tubular atrophy (**asterisk**) in BX471-treated mice (**G**) and vehicle-treated controls (**H**) at day 12 after UUO. Renal sections were stained with Masson's trichrome (MT) to detect interstitial collagen (blue) in vehicle-treated mice (**I**) and BX471-treated mice (**J**) at day 12 after UUO. CCL5 expression was reduced in BX471-treated mice (**K**) at day 5 after obstruction [vehicle-treated mice (**L**)] and localized mainly to cortical tubules. Original magnifications: ×400 (**A**, **B**, **E**, and **F**); ×250 (**I–L**).

and sham-operated controls (Figure 3A). BX471-treated mice showed a decrease in interstitial fibrosis by 39% at day 5 after UUO (166 ± 4.4 versus 272 ± 15, $P < 0.05$) and by 38% at day 12 after UUO (372 ± 16 versus 597 ± 15, $P < 0.05$) when compared with vehicle-treated mice (Figures 2, I and J, and 3A). In intact opposite controls and sham-operated kidneys, there was no increase in interstitial collagen deposition (Figure 3A). We questioned whether a reduction in macrophage recruitment would affect the expression of the profibrotic cytokine TGF-β_1 in obstructed kidneys (Figure 3B). Quantitative RT-PCR demonstrated a significant increase of TGF-β_1 mRNA in obstructed kidneys when compared with sham-operated controls. By contrast, TGF-β_1 mRNA expression was completely normalized in BX471-treated mice with UUO at day 5 after obstruction (Figure 3B). In addition, collagen I mRNA expression was significantly diminished in obstructed kidneys of BX471-treated mice compared with vehicle controls at day 12 after UUO (Figure 3C) ($P < 0.05$).

Renal Chemokine Production

Because locally expressed chemokines mediate renal leukocyte recruitment, we investigated whether BX471 treatment affected the local production of CC-chemokines in obstructed kidneys (Figure 3D). We performed real-time RT-PCR for CCL5, CCL3, CCL4, and CCL2 mRNA on total renal isolates from vehicle- and BX471-treated mice at 5 and 12 days after UUO. CCL5, CCL3, and CCL4 were significantly up-regulated after UUO, with CCL5 being the most prominent chemokine in obstructed kidneys (4.5-fold change over sham-operated control at day 5 and 14.8-fold change at day 12 after UUO). BX471 reduced CCL5 mRNA by 62% (1.7-fold change versus 4.5-fold change over sham-operated control, $P < 0.05$) and completely prevented the increase in CCL3 (onefold versus 2.4-fold change, $P < 0.05$) and CCL4 (onefold versus 2.5-fold change, $P < 0.05$) at day 5 after UUO (Figure 3D). Notably, CCL2 mRNA remained unaffected by UUO in neonatal mice and may be differentially regulated in neonatal and adult mice with UUO. Together, these data suggest that BX471 modulates the expression of CC-chemokines in UUO-kidneys, either by impairing recruitment of chemokine-producing cells to the kidney or possibly by directly inhibiting chemokine production in resident renal macrophages. Interestingly, immunohistochemistry for CCL5 revealed a strong signal in cortical tubular cells and to a lesser extent in the interstitium at day 5 after obstruction (Figure 2, K and L). CCL5 protein

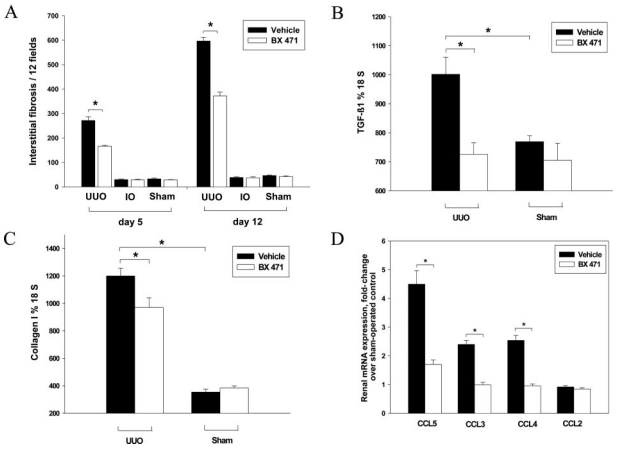

Figure 3. A: Morphometric analysis of interstitial fibrosis (Masson trichrome staining) at 5 and 12 days after surgery in BX471-treated mice (day 2 to day 14 of life) and vehicle-treated controls. Twelve fields were analyzed. UUO, obstructed kidney; IO, intact opposite kidney; sham, sham-operated control kidneys. Data are given as mean ± SE ($n = 8$ in each group). Quantitative real-time RT-PCR for TGF-β_1 (**B**) (day 5 after UUO); collagen Iα (**C**) (day 12 after UUO); and chemokines CCL5, CCL3, CCL4, and CCL2 (**D**) (day 5 after UUO) in obstructed kidneys and sham-operated controls of vehicle- and BX471-treated mice. mRNA expression was normalized to ribosomal 18S expression as described in Materials and Methods. $^*P < 0.05$. Original magnifications, ×400.

expression was attenuated by BX471 treatment, as evidenced by decreased staining of CCL5 in the UUO-kidney at day 5 after UUO (Figure 2, K and L).

Epithelial Mesenchymal Transition (EMT)

We questioned whether the EMT transcriptional regulators Snail1 and Snail2/Slug and mesenchymal markers [vimentin and smooth muscle actin (SMA)] were regulated by UUO in neonatal mice, as well as by leukocyte recruitment. BX471 was used to block leukocyte infiltration. As shown in Figure 4, Snail1 and Snail2/Slug mRNA

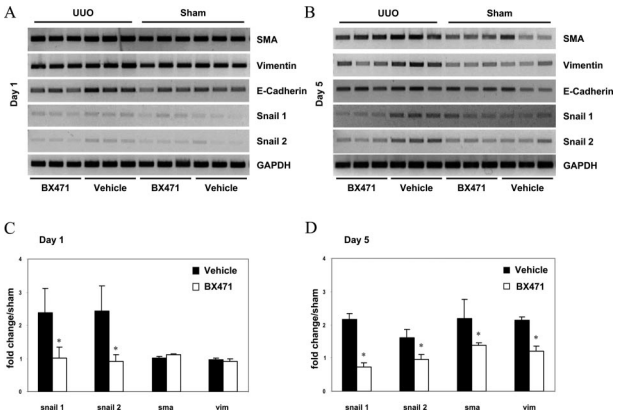

Figure 4. UUO-dependent Snail1 and Snail2/Slug mRNA is attenuated by BX471. Neonatal mice were subjected to UUO or sham operation and treated with BX471 or vehicle, as indicated. Whole kidney extracts were prepared, total RNA isolated, and RT-PCR for the indicated genes performed. RNA profiles were obtained in cohorts that were harvested at days 1 (**A**) and 5 (**B**) after UUO or sham operation, respectively. Independent RT-PCR with an $n = 3$ per group were performed at least one time, and representative gels are depicted. Densitometric analysis was performed to quantify gene expression patterns obtained at days 1 (**C**) and 5 (**D**) after UUO. Values for Snail1, Snail2/Slug, SMA, and vimentin were derived by referring to GAPDH expression in the same samples. $^*P < 0.05$.

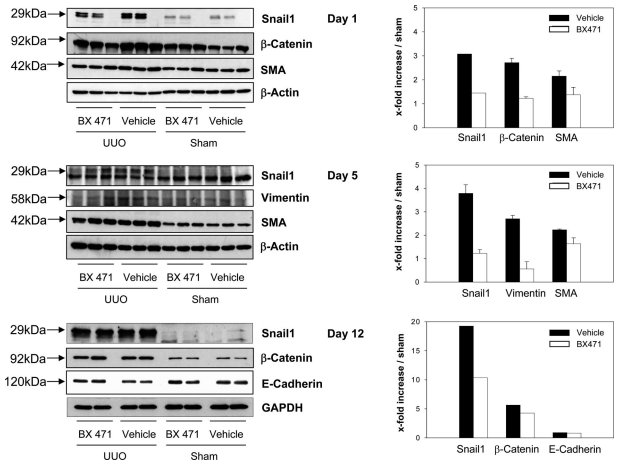

Figure 5. EMT markers are induced by UUO and attenuated by BX471. Protein expression of Snail1, active β-catenin, E-cadherin, vimentin, and SMA. Neonatal mice were subjected to UUO or sham operation and treated with BX471. Whole kidneys were processed for Western blot analysis as described in Materials and Methods at days 1, 5, and 12 after obstruction. Densitometric analysis was performed to quantify protein expression obtained at days 1, 5, and 12 after UUO.

was rapidly increased in obstructed kidneys, as early as 1 day after UUO. In the presence of BX471, this increased Snail1 and Snail2/Slug mRNA was completely attenuated (Figure 4, C and D). Increased expression of SMA and vimentin, two mesenchymal markers, became evident only at day 5 after UUO, but their expression was also attenuated by BX471 treatment (Figure 4D). Snail1 and Snail2/Slug expression preceded the induction of SMA and vimentin, indicating that both were early markers of EMT. Total E-cadherin mRNA abundance in the kidney remained unchanged by BX471-treatment and UUO surgery. On the protein level, we found a strong increase in Snail1 expression in obstructed kidneys at 1, 5, and 12 days after obstruction (Figure 5). In the presence of BX471, this increased Snail1 expression was markedly reduced (Figure 5). The reduction in Snail1 was stronger at the mRNA than at the protein level. Active β-catenin and vimentin, both markers for EMT, were reduced in BX471-treated mice with UUO. The myofibroblast marker SMA showed a tendency of lower expression levels in obstructed kidneys of BX471-treated mice (Figure 5). To determine whether phenotypic changes occurred in UUO kidneys, we examined the expression of E-cadherin, a hallmark of epithelium by immunofluorescence. As depicted in Figure 6, localization of E-cadherin was mainly observed in the expected intercellular junction area of renal tubules. After UUO, E-cadherin expression strongly decreased in obstructed kidneys throughout time. By contrast, BX471 treatment reduced loss of E-cadherin in UUO kidneys. Together, these results suggest that UUO induced EMT, which was significantly attenuated by BX471. To investigate the localization of Snail1, we stained control and UUO kidneys, vehicle- and BX471-treated, with antibodies specific for SMA and Snail1 (Figure 7). As early as 5 days after UUO, kidneys demonstrated relatively increased SMA staining in the medulla, reflecting the persistence of an immature phenotype of the obstructed kidney. Snail1-positive staining

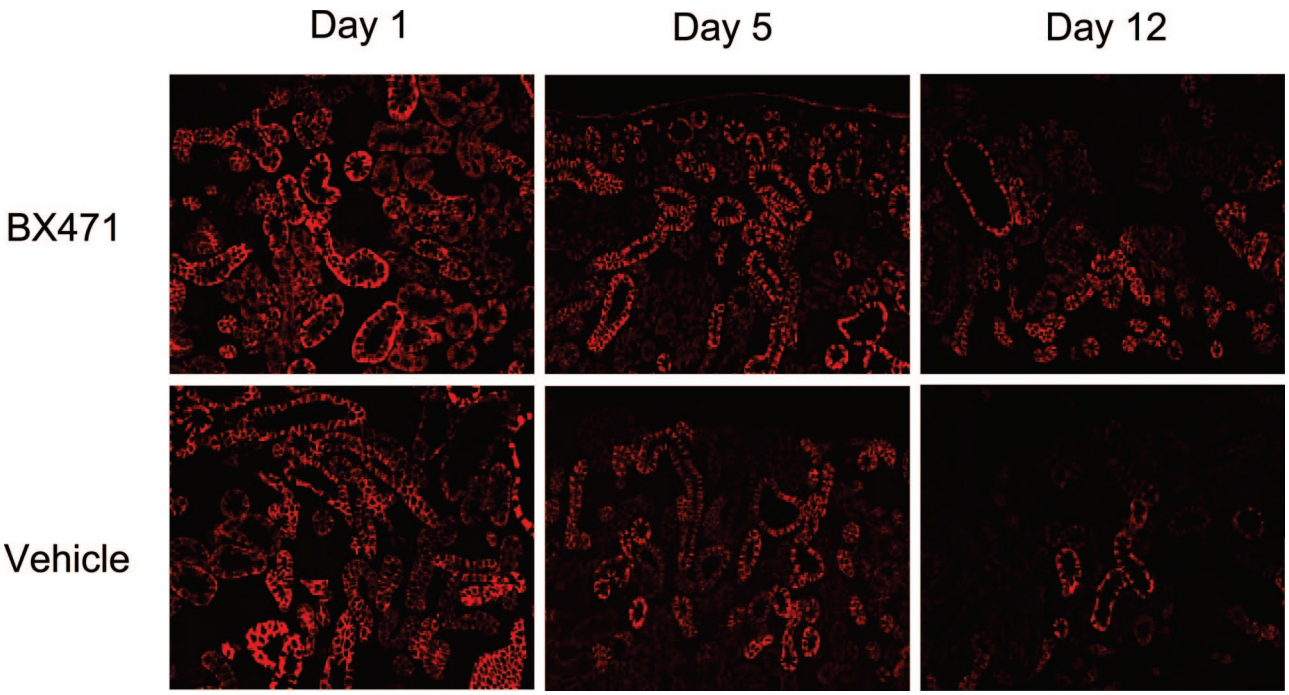

Figure 6. Immunofluorescence of E-cadherin in obstructed kidneys at days 1, 5, and 12 after obstruction. Mice were treated with BX471 (day 2 to day 14 of life) or vehicle. UUO induced EMT and loss of E-cadherin. BX471 reduced the loss of E-cadherin and the severity of EMT in obstructed kidneys.

increased in tubular epithelial cells of the cortex and medulla (Figure 7). Protein expression of SMA and Snail1 was attenuated by BX471 treatment, as evidenced by decreased staining of SMA and Snail1 in the medulla and cortex, respectively (Figure 7).

Pharmacokinetics of BX471

BX471 concentration in plasma was analyzed by high-performance liquid chromatography and mass spectrometry.[5,39] As shown in Figure 8A, BX471 plasma levels peaked after 6 hours at ~7.0 μmol/L, declined to 4.7 μmol/L after 12 hours, and dropped to 0.25 μmol/L at 24 hours after injection. Drug concentrations of 2 to 5 μmol/L are sufficient for effective CCR-1 blockade. Based on these data we decided to dose the animals subcutaneously once a day with 100 mg/kg body weight of BX471. BX471 administration did not induce changes in body weight gain (see Figure 8B).

Discussion

This study addresses the role of inflammatory leukocytes in EMT in neonatal obstructive nephropathy. Snail1, a key regulator of EMT, was rapidly increased after neonatal UUO as well as Snail2/Slug, which belongs to the snail family of zinc-finger transcription factors. Both are strong repressors of transcription of the E-cadherin gene and are implicated in pathological EMT.[13,40,41] In the presence of BX471, the increased Snail1 and Snail2/Slug expression was completely attenuated, suggesting a close relationship between the degree of leukocyte infiltration and EMT. In addition, BX471-treated mice exhibited reduced levels of β-catenin, SMA, and vimentin expression. Furthermore, renal protein expression of SMA and Snail1 was attenuated by BX471, as evidenced by decreased staining of SMA-positive myofibroblasts and reduced tubular Snail1 expression in the medulla and cortex of the obstructed kidney, respectively. In addition, the loss of E-cadherin after UUO was reduced in BX471-treated mice. Our data suggest that infiltrating leukocytes induce EMT in neonatal UUO, thereby enhancing interstitial fibrosis in obstructive nephropathy.

Macrophages and Interstitial Fibrosis

Several investigators have used different methods to address the role of macrophages in EMT and interstitial fibrosis, with inconsistent results. Exogenous wild-type monocytes, either co-cultured with renal tubular epithelial cells *in vitro* or transplanted into the obstructed kidney in the UUO model *in vivo*, facilitated EMT, providing evidence that the monocyte influx in UUO contributes to interstitial fibrosis.[42] In a murine model of crescentic glomerulonephritis, depletion of macrophages markedly reduced the amount of renal myofibroblasts and interstitial fibrosis.[11] Furthermore, in the presence of macrophages, interstitial myofibroblasts exhibited increased levels of both proliferation and apoptosis, suggesting that macrophages act to support the population of myofibroblasts.[11] Our pharmacological blockade of leukocyte recruitment confirms and extends the previously suggested role of infiltrating leukocytes in EMT and interstitial fibrosis in the obstructed kidney.

In advanced liver fibrosis macrophage depletion resulted in reduced scarring and fewer myofibroblasts but

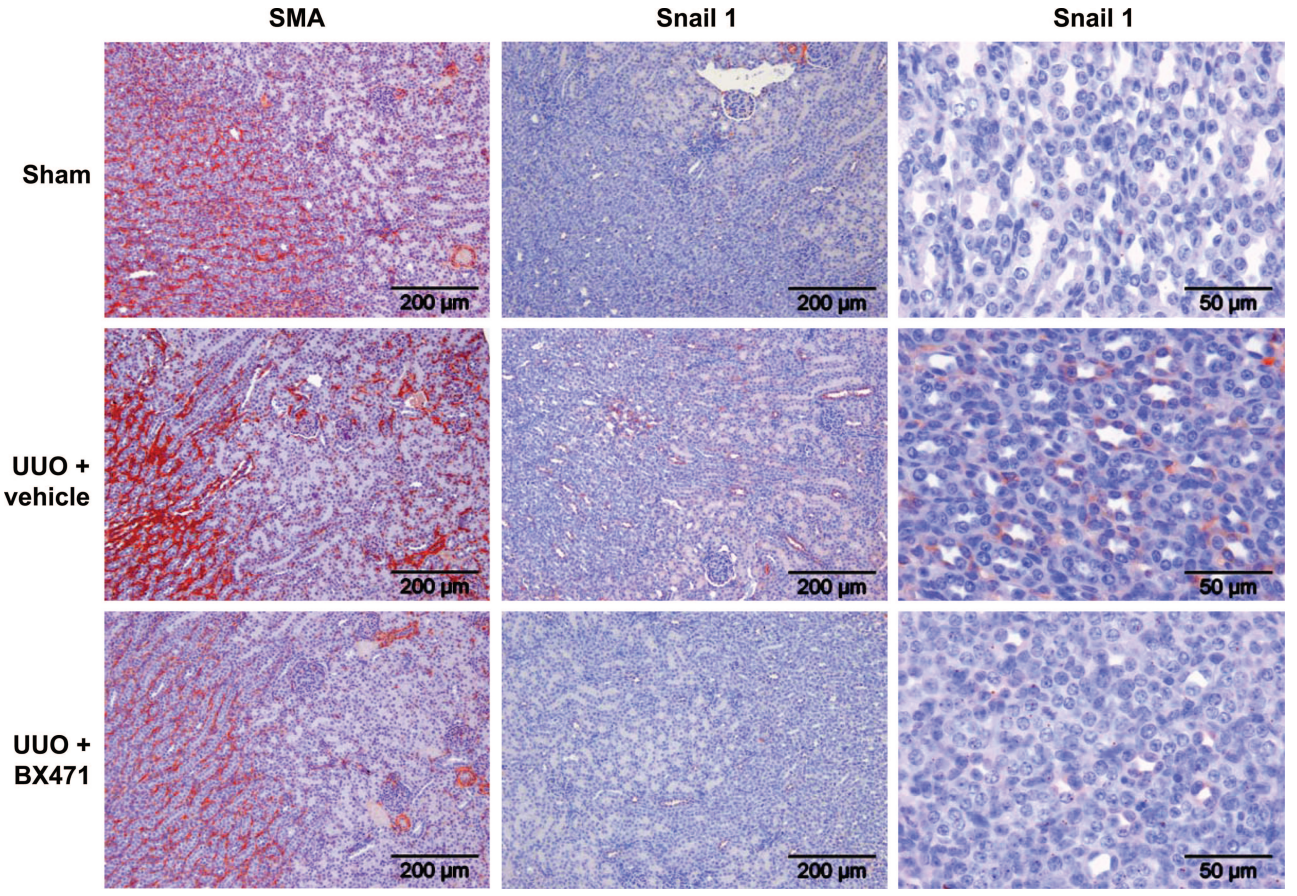

Figure 7. Protein expression of SMA and Snail1 is induced by UUO and attenuated by BX471. Neonatal mice were subjected to UUO or sham operation and treated with BX471. Whole kidney sections were prepared and processed for immunostaining of SMA and Snail1 as described in Materials and Methods at day 5 after surgery. Immunolocalization of SMA in sham, UUO, and UUO + BX471 groups are depicted in the left column, and corresponding stainings of Snail1 in the middle column. The right column depicts higher resolution pictures of Snail1 staining. Original magnifications: ×100 (left and middle columns); ×400 (right column).

compromised matrix degradation during recovery.[43] In a mouse model of UUO, adoptive transfer of bone marrow-derived macrophages after pharmacological depletion of leukocytes increased the numbers of interstitial macrophages and reduced renal fibrosis, suggesting that macrophages facilitate tissue repair at late stages of UUO.[44] These studies provide evidence that functionally distinct subpopulations of macrophages exist in the same tissue and that these macrophages perform both injury-inducing and repair-promoting tasks in different models of inflammation. In our study of neonatal UUO, there may be different populations of macrophages serving different functions simultaneously. Besides reducing leukocyte infiltration, BX471 may have an additional effect on the macrophage phenotype presenting in the obstructed kidney.

Macrophages and Myofibroblasts

In vitro studies addressing interactions between macrophages and myofibroblasts show that macrophages are capable of inducing myofibroblast proliferation, apoptosis, abnormal extracellular matrix synthesis, and matrix degradation through production of nitric oxide, tumor necrosis factor-α, and up-regulation of collagenases and other metalloproteinases.[11,43,45] Recently, it has been demonstrated that activated monocyte supernatant and oncostatin M, a cytokine released by activated mononuclear cells, induce EMT in tubular cells.[46,47] In hepatocytes, activated macrophage-conditioned medium stimulated EMT and led to enhanced migratory and invasive activities of HepG2 cells.[48] These observations support our hypothesis that leukocytes mediate EMT in neonatal UUO. However, the signaling pathways of EMT induction are not yet clear at present.

EMT Signaling

Many cytokines, growth factors, and adhesion molecules associated with UUO and macrophage infiltration regulate EMT.[46,47] Among them, TGF-β_1 seems to be critical. This is confirmed by the finding that neutralizing antibodies against TGF-β_1 prevent EMT in tubular epithelial cells.[49] Mice lacking Smad3, a key signaling intermediate downstream of the TGF-β receptors, are protected against tubulointerstitial fibrosis after UUO as evidenced by blocking of EMT and abrogation of monocyte influx.[42] However, immunoneutralization of TGF-β_1 resulted only in a 20% inhibition of EMT, suggesting that multiple cytokines, released by macrophages and tubular cells, si-

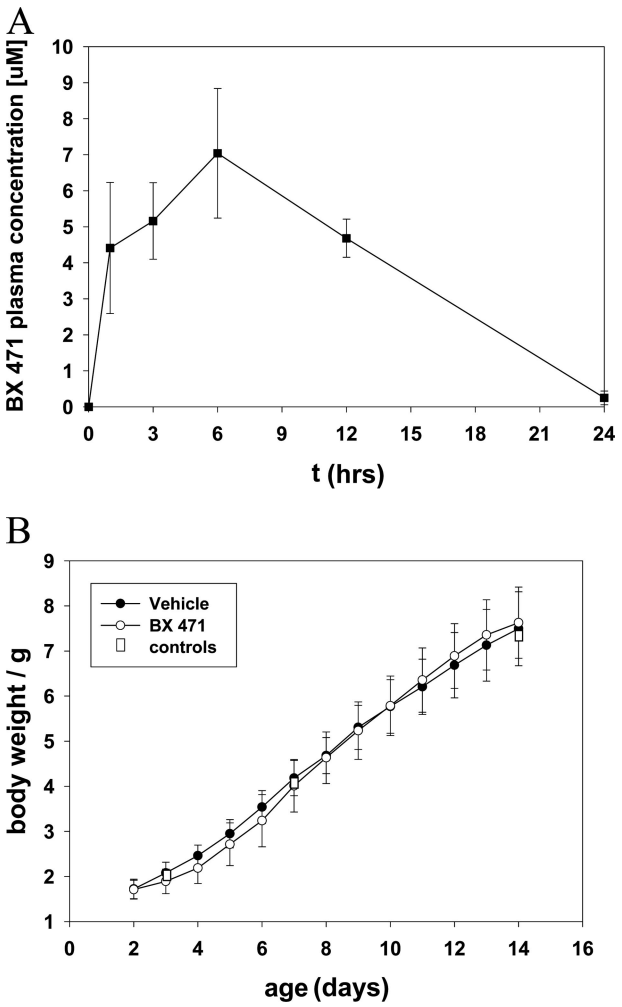

Figure 8. Pharmacokinetics of BX471 in neonatal mice. Neonatal mice (n = 4 at each time point) received a single dose (100 mg/kg) of BX471 in propylene glycol. **A:** Plasma concentrations of BX471 after subcutaneous injection. Blood plasma levels were measured as described previously.[39] Data are the mean ± SD. Drug concentrations of 2 to 5 μmol/L are sufficient for effective CCR-1 blockade. **B:** Body weight of neonatal mice with BX471, vehicle, or without treatment (controls) from day 2 to day 14 of life, P = NS.

multaneously activate a number of cellular receptors, finally leading to transcriptional regulation of EMT.[46] Our data show accordingly that blockade of leukocyte recruitment reduced expression of TGF-β_1 and mesenchymal markers but did not completely prevent cytokine release and EMT in neonatal UUO.

Macrophages and Tubular Apoptosis

Tubular apoptosis is a major cause of cell death in UUO.[50] In the neonatal kidney, tubular apoptosis increases in response to UUO to a much greater extent than in the adult kidney.[51] We show that the decrease in the number of infiltrating cells in BX471-treated mice was associated with a marked reduction in tubular apoptosis and tubular atrophy after UUO. The strong anti-apoptotic effect of CCR-1 antagonism in tubular cells was closely related to the degree of inflammatory macrophage infiltration, which is in line with previous reports on macrophage-induced apoptosis in tubular epithelial cells.[6,9,52] Tubular apoptosis after UUO is promoted by a number of stimuli, including cytokines (TGF-β_1, tumor necrosis factor-α) and oxidative stress. Several studies have shown that reducing initial cell death, by either neutralizing the activity of proapoptotic molecules or supplementing with prosurvival factors, effectively prevents inflammation, further cell death, and fibrosis.[50] Our results in neonatal UUO are in agreement with those observations. Furthermore, our data suggest that the reduction of tubular apoptosis is likely to limit the generation of signals released from dying cells that would otherwise continue to stimulate the inflammatory response as we have shown for the expression of CCL5 in tubular cells.

Leukocytes and Chemokine Expression

In our model, blockade of leukocyte recruitment by BX471 markedly reduced the mRNA expression of CCL3, CCL4, and CCL5 as well as the amount of CCL5-positive cells in obstructed kidneys. This suggests that BX471 modulates the expression of CCL5 in UUO either by blocking recruitment of CCL5-producing cells or possibly by directly inhibiting CCL5 production in renal macrophages. The latter is supported by recent *in vitro* data, showing that CCR-1 ligation by its ligand CCL3 contributes to macrophage CCL5 production, which may then facilitate additional leukocyte recruitment, local inflammation, and tubulointerstitial injury.[53] Moreover, chemokines may not only promote leukocyte recruitment but may also modulate the immune response and the phenotype of infiltrating cells during inflammation. Chemokines trigger monocyte differentiation into a dendritic cell phenotype,[54] induce activation and proliferation of T cells.[55] and costimulate T-lymphocyte function.[56] Therefore it is likely that the activation status of the infiltrating leukocyte in BX471- and vehicle-treated mice may contribute differentially to the tubulointerstitial injury after UUO.

Together these data argue for a significant contribution of infiltrating leukocytes to EMT and the progression of interstitial fibrosis in congenital obstructive nephropathy. We show for the first time that EMT is present in the developing kidney with UUO and that leukocytes are key effectors of disease progression by modulating apoptosis, EMT, and partial interstitial fibrosis, suggesting that inflammatory macrophages may represent a potential target for therapeutic intervention in obstructive nephropathy.

References

1. Seikaly MG, Ho PL, Emmett L, Fine RN, Tejani A: Chronic renal insufficiency in children: the 2001 Annual Report of the NAPRTCS. Pediatr Nephrol 2003, 18:796–804
2. Klahr S, Morrissey J: Obstructive nephropathy and renal fibrosis. Am J Physiol 2002, 283:F861–F875
3. Bascands JL, Schanstra JP: Obstructive nephropathy: insights from genetically engineered animals. Kidney Int 2005, 68:925–937
4. Chevalier RL: Perinatal obstructive nephropathy. Semin Perinatol 2004, 28:124–131
5. Anders HJ, Vielhauer V, Frink M, Linde Y, Cohen CD, Blattner SM, Kretzler M, Strutz F, Mack M, Grone HJ, Onuffer J, Horuk R, Nelson PJ, Schlondorff D: A chemokine receptor CCR-1 antagonist reduces

renal fibrosis after unilateral ureter ligation. J Clin Invest 2002, 109:251–259
6. Lange-Sperandio B, Cachat F, Thornhill BA, Chevalier RL: Selectins mediate macrophage infiltration in obstructive nephropathy in newborn mice. Kidney Int 2002, 61:516–524
7. Lange-Sperandio B, Schimpgen K, Rodenbeck B, Chavakis T, Bierhaus A, Nawroth P, Thornhill B, Schaefer F, Chevalier RL: Distinct roles of Mac-1 and its counter-receptors in neonatal obstructive nephropathy. Kidney Int 2006, 69:81–88
8. Sean Eardley K, Cockwell P: Macrophages and progressive tubulointerstitial disease. Kidney Int 2005, 68:437–455
9. Lenda DM, Kikawada E, Stanley ER, Kelley VR: Reduced macrophage recruitment, proliferation, activation in colony-stimulating factor-1-deficient mice results in decreased tubular apoptosis during renal inflammation. J Immunol 2003, 170:3254–3262
10. Lange-Sperandio B, Fulda S, Vandewalle A, Chevalier RL: Macrophages induce apoptosis in proximal tubule cells. Pediatr Nephrol 2003, 18:335–341
11. Duffield JS, Tipping PG, Kipari T, Cailhier JF, Clay S, Lang R, Bonventre JV, Hughes J: Conditional ablation of macrophages halts progression of crescentic glomerulonephritis. Am J Pathol 2005, 167:1207–1219
12. Chow FY, Nikolic-Paterson DJ, Atkins RC, Tesch GH: Macrophages in streptozotocin-induced diabetic nephropathy: potential role in renal fibrosis. Nephrol Dial Transplant 2004, 19:2987–2996
13. Kalluri R, Neilson EG: Epithelial-mesenchymal transition and its implications for fibrosis. J Clin Invest 2003, 112:1776–1784
14. Neilson EG: Setting a trap for tissue fibrosis. Nat Med 2005, 11:373–374
15. Lee JM, Dedhar S, Kalluri R, Thompson EW: The epithelial-mesenchymal transition: new insights in signaling, development, and disease. J Cell Biol 2006, 172:973–981
16. Roxburgh SA, Murphy M, Pollock CA, Brazil DP: Recapitulation of embryological programmes in renal fibrosis—the importance of epithelial cell plasticity and developmental genes. Nephron Physiol 2006, 103:139–148
17. Iwano M, Plieth D, Danoff TM, Xue C, Okada H, Neilson EG: Evidence that fibroblasts derive from epithelium during tissue fibrosis. J Clin Invest 2002, 110:341–350
18. Zeisberg M, Kalluri R: The role of epithelial-to-mesenchymal transition in renal fibrosis. J Mol Med 2004, 82:175–181
19. Barrallo-Gimeno A, Nieto MA: The Snail genes as inducers of cell movement and survival: implications in development and cancer. Development 2005, 132:3151–3161
20. Carrozzino F, Soulie P, Huber D, Mensi N, Orci L, Cano A, Feraille E, Montesano R: Inducible expression of Snail selectively increases paracellular ion permeability and differentially modulates tight junction proteins. Am J Physiol 2005, 289:C1002–C1014
21. Parent AE, Choi C, Caudy K, Gridley T, Kusewitt DF: The developmental transcription factor slug is widely expressed in tissues of adult mice. J Histochem Cytochem 2004, 52:959–965
22. Medici D, Hay ED, Goodenough DA: Cooperation between snail and LEF-1 transcription factors is essential for TGF-β1-induced epithelial-mesenchymal transition. Mol Biol Cell 2006, 17:1871–1879
23. Liu Y: Epithelial to mesenchymal transition in renal fibrogenesis: pathologic significance, molecular mechanism, and therapeutic intervention. J Am Soc Nephrol 2004, 15:1–12
24. Thiery JP, Chopin D: Epithelial cell plasticity in development and tumor progression. Cancer Metastasis Rev 1999, 18:31–42
25. Docherty NG, O'Sullivan OE, Healy DA, Murphy M, O'Neill AJ, Fitzpatrick JM, Watson RW: TGF-β1-induced EMT can occur independently of its proapoptotic effects and is aided by EGF receptor activation. Am J Physiol 2006, 290:F1202–F1212
26. Shin GT, Kim WH, Yim H, Kim MS, Kim H: Effects of suppressing intrarenal angiotensinogen on renal transforming growth factor-beta1 expression in acute ureteral obstruction. Kidney Int 2005, 67:897–908
27. Fukasawa H, Yamamoto T, Togawa A, Ohashi N, Fujigaki Y, Oda T, Uchida C, Kitagawa K, Hattori T, Suzuki S, Kitagawa M, Hishida A: Ubiquitin-dependent degradation of SnoN and Ski is increased in renal fibrosis induced by obstructive injury. Kidney Int 2006, 69:1733–1740
28. Mackay CR: Chemokines: immunology's high impact factors. Nat Immunol 2001, 2:95–101
29. Segerer S, Nelson PJ, Schlondorff D: Chemokines, chemokine receptors, and renal disease: from basic science to pathophysiologic and therapeutic studies. J Am Soc Nephrol 2000, 11:152–176
30. Anders HJ, Ninichuk V, Schlondorff D: Progression of kidney disease: blocking leukocyte recruitment with chemokine receptor CCR1 antagonists. Kidney Int 2006, 69:29–32
31. Miyasaka M, Tanaka T: Lymphocyte trafficking across high endothelial venules: dogmas and enigmas. Nat Rev Immunol 2004, 4:360–370
32. Chevalier RL, Peters CA: Congenital urinary tract obstruction: proceedings of the State-Of-The-Art Strategic Planning Workshop-National Institutes of Health, Bethesda, MD, 11–12 March 2002. Pediatr Nephrol 2003, 18:576–606
33. Horuk R: BX471: a CCR1 antagonist with anti-inflammatory activity in man. Mini Rev Med Chem 2005, 5:791–804
34. Ninichuk V, Anders HJ: Chemokine receptor CCR1: a new target for progressive kidney disease. Am J Nephrol 2005, 25:365–372
35. Vielhauer V, Berning E, Eis V, Kretzler M, Segerer S, Strutz F, Horuk R, Grone HJ, Schlondorff D, Anders HJ: CCR1 blockade reduces interstitial inflammation and fibrosis in mice with glomerulosclerosis and nephrotic syndrome. Kidney Int 2004, 66:2264–2278
36. Liang M, Mallari C, Rosser M, Ng HP, May K, Monahan S, Bauman JG, Islam I, Ghannam A, Buckman B, Shaw K, Wei GP, Xu W, Zhao Z, Ho E, Shen J, Oanh H, Subramanyam B, Vergona R, Taub D, Dunning L, Harvey S, Snider RM, Hesselgesser J, Morrissey MM, Perez HD: Identification and characterization of a potent, selective, and orally active antagonist of the CC chemokine receptor-1. J Biol Chem 2000, 275:19000–19008
37. Cachat F, Lange-Sperandio B, Chang AY, Kiley SC, Thornhill BA, Forbes MS, Chevalier RL: Ureteral obstruction in neonatal mice elicits segment-specific tubular cell responses leading to nephron loss. Kidney Int 2003, 63:564–575
38. Chevalier RL, Thornhill BA, Chang AY, Cachat F, Lackey A: Recovery from release of ureteral obstruction in the rat: relationship to nephrogenesis. Kidney Int 2002, 61:2033–2043
39. Fern RJ, Yesko CM, Thornhill BA, Kim HS, Smithies O, Chevalier RL: Reduced angiotensinogen expression attenuates renal interstitial fibrosis in obstructive nephropathy in mice. J Clin Invest 1999, 103: 39–46
40. Cano A, Perez-Moreno MA, Rodrigo I, Locascio A, Blanco MJ, del Barrio MG, Portillo F, Nieto MA: The transcription factor snail controls epithelial-mesenchymal transitions by repressing E-cadherin expression. Nat Cell Biol 2000, 2:76–83
41. Thuault S, Valcourt U, Petersen M, Manfioletti G, Heldin CH, Moustakas A: Transforming growth factor-β employs HMGA2 to elicit epithelial-mesenchymal transition. J Cell Biol 2006, 174:175–183
42. Sato M, Muragaki Y, Saika S, Roberts AB, Ooshima A: Targeted disruption of TGF-β1/Smad3 signaling protects against renal tubulointerstitial fibrosis induced by unilateral ureteral obstruction. J Clin Invest 2003, 112:1486–1494
43. Duffield JS, Forbes SJ, Constandinou CM, Clay S, Partolina M, Vuthoori S, Wu S, Lang R, Iredale JP: Selective depletion of macrophages reveals distinct, opposing roles during liver injury and repair. J Clin Invest 2005, 115:56–65
44. Nishida M, Okumura Y, Fujimoto S, Shiraishi I, Itoi T, Hamaoka K: Adoptive transfer of macrophages ameliorates renal fibrosis in mice. Biochem Biophys Res Commun 2005, 332:11–16
45. Duffield JS: The inflammatory macrophage: a story of Jekyll and Hyde. Clin Sci (Lond) 2003, 104:27–38
46. Nightingale J, Patel S, Suzuki N, Buxton R, Takagi KI, Suzuki J, Sumi Y, Imaizumi A, Mason RM, Zhang Z: Oncostatin M, a cytokine released by activated mononuclear cells, induces epithelial cell-myofibroblast transdifferentiation via Jak/Stat pathway activation. J Am Soc Nephrol 2004, 15:21–32
47. Patel S, Takagi KI, Suzuki J, Imaizumi A, Kimura T, Mason RM, Kamimura T, Zhang Z: RhoGTPase activation is a key step in renal epithelial mesenchymal transdifferentiation. J Am Soc Nephrol 2005, 16:1977–1984
48. Lin CY, Lin CJ, Chen KH, Wu JC, Huang SH, Wang SM: Macrophage activation increases the invasive properties of hepatoma cells by destabilization of the adherens junction. FEBS Lett 2006, 580: 3042–3050
49. Wang W, Koka V, Lan HY: Transforming growth factor-β and Smad signalling in kidney diseases. Nephrology (Carlton) 2005, 10:48–56

50. Docherty NG, O'Sullivan OE, Healy DA, Fitzpatrick JM, Watson RW: Evidence that inhibition of tubular cell apoptosis protects against renal damage and development of fibrosis following ureteric obstruction. Am J Physiol 2006, 290:F4–F13
51. Chevalier RL, Thornhill BA, Chang AY, Cachat F, Lackey A: Recovery from release of ureteral obstruction in the rat: relationship to nephrogenesis. Kidney Int 2002, 61:2033–2043
52. Kipari T, Cailhier JF, Ferenbach D, Watson S, Houlberg K, Walbaum D, Clay S, Savill J, Hughes J: Nitric oxide is a important mediator of renal tubular epithelial cell death in vitro and in murine experimental hydronephrosis. Am J Pathol 2006, 169:388–399
53. Ninichuk V, Gross O, Reichel C, Khandoga A, Pawar RD, Ciubar R, Segerer S, Belemezova E, Radomska E, Luckow B, De Lema GP, Murphy PM, Gao JL, Henger A, Kretzler M, Horuk R, Weber M, Krombach F, Schlondorff D, Anders HJ: Delayed chemokine receptor 1 blockade prolongs survival in collagen 4A3-deficient mice with Alport disease. J Am Soc Nephrol 2005, 16:977–985
54. Wang J, Alvarez R, Roderiquez G, Guan E, Caldwell Q, Wang J, Phelan M, Norcross MA: CpG-independent synergistic induction of beta-chemokines and a dendritic cell phenotype by orthophosphorothioate oligodeoxynucleotides and granulocyte-macrophage colony-stimulating factor in elutriated human primary monocytes. J Immunol 2005, 174:6113–6121
55. Guo Z, Zhang M, Tang H, Cao X: Fas signal links innate and adaptive immunity by promoting dendritic cell secretion of CC and CXC chemokines. Blood 2005,106:2033–2041
56. Taub DD, Turcovski-Corrales SM, Key ML, Longo DL, Murphy WJ: Chemokines and T lymphocyte activation: I. Beta chemokines costimulate human T lymphocyte activation in vitro. J Immunol 1996, 156:2095–2103